Am J Transl Res 2025;17(7):5355-5370
www.ajtr.org /ISSN:1943-8141/AJTR0166385

Original Article

GSK3β serves as a novel therapeutic target in patients with type 2 diabetes mellitus complicated by colorectal cancer

Jixuan Lu[1], Lijie Sun[1], Xinyu Li[1], Yan Cao[1], Jie Gao[1], Dengju Yao[2], Xiaorong Zhan[1]

[1]Department of Endocrinology, The First Affiliated Hospital of Harbin Medical University, Harbin 150001, Heilongjiang, China; [2]School of Computer Science and Technology, Harbin University of Science and Technology, Harbin 150080, Heilongjiang, China

Received May 27, 2025; Accepted June 28, 2025; Epub July 15, 2025; Published July 30, 2025

Abstract: In clinical practice, tumor occurrence and progression appear to be more frequent and rapid in patients with type 2 diabetes mellitus (T2DM) compared to non-diabetic individuals. Epidemiological studies have confirmed that the incidence of colorectal cancer (CRC) is relatively higher in patients with T2DM. However, the key candidate regulatory factors that mediate and drive the concurrent development and progression of T2DM and CRC remain unclear. Analysis using the Significant Bias Evaluation Method on clinical data revealed that patients with T2DM have a higher propensity for developing lung cancer, colorectal cancer, and breast cancer. Further analysis of the key factors associated with T2DM and related tumors identified GSK3β as a potential key regulatory factor in CRC development in T2DM patients, through differential expression analysis using the limma package on real-world data. Western blot and qRT-PCR validation revealed that, compared to the non-insulin-resistant HT29 CRC cell line group, the mRNA and protein expression levels of GSK3β were significantly elevated in the insulin-resistant group. Similarly, the mRNA and protein expression levels of factors associated with the GSK3β-β-catenin-CyclinD1/cMyc pathway were also upregulated. Furthermore, when GSK3β was silenced or overexpressed, the proliferative effect of tumor cells was markedly reduced or increased, respectively. In summary, GSK3β is upregulated in T2DM patients with CRC and contributes to tumor progression. GSK3β holds promise as a novel therapeutic target for the treatment of patients with T2DM complicated by CRC, potentially providing a solution to address clinical challenges.

Keywords: Type 2 diabetes mellitus, colorectal cancer, GSK3β, bioinformation

Introduction

Type 2 diabetes mellitus (T2DM) is a complex metabolic disorder caused by multiple etiologies and is often accompanied by numerous complications, including malignant tumors [1, 2]. Clinical observations suggest that tumor incidence and progression of tumors are both higher and more rapid in T2DM patients compared to non-diabetic individuals. In 2021, Pearson-Stuttard J [3] published an epidemiological study in *The Lancet Diabetes & Endocrinology*, which followed over 200,000 diabetic patients for 18 years. The results showed that the proportion of deaths attributable to cancer was significantly higher in diabetic patients compared with non-diabetic individuals (9.0% vs. 6.5%), representing an approximate 50% relative increase in cancer-related mortality. Notably, cancer has become the leading cause of death among people with diabetes in England.

Epidemiological evidence shows that patients with T2DM have a higher the incidence of several malignancies, including colorectal, liver, gastric, pancreatic, lung, bladder, prostate, breast, cervical, and endometrial cancers. A 2023 Chinese epidemiological study [4] involving 46,066 T2DM patients demonstrated that T2DM is significant risk factor for cancer, with malignancies accounting for the largest proportion (32.14%), primarily colorectal cancer (CRC) and gastric cancer. Another large-scale prospective study on chronic diseases in China, involving 500,000 participants, reported that

https://doi.org/10.62347/TQUD3910

the risk of CRC in diabetic individuals was 44% higher than in the general population [5]. Additionally, the incidence of CRC in China has increased markedly, now ranking the fourth most common malignant tumor and the fifth leading cause of cancer-related death [6]. In 2024, an article published in *Nature* by Luís Nunes [7] reported that approximately 20% of CRC patients present with metastasis at diagnosis, and an additional 20% develop metastasis subsequently, underscoring the public health burden posed by CRC. Early detection and treatment of CRC are critical to improving cure rates, reducing recurrence rates, enhancing quality of life, and lowering medical costs [8]. The incidence of CRC in T2DM patients is increasing annually. However, the mechanisms linking these two diseases remain unclear. As T2DM is a major risk factor for cancer, it is important to identify whether specific molecular mediators drive CRC development in this population. Determining the key regulatory factors that contribute to CRC progression in T2DM patients may provide new insights into novel biological markers and therapeutic targets, ultimately offering new strategies for prevention and treatment of CRC in this population.

Materials and methods

Bioinformatic technology

Significant bias evaluation method for assessing cancer susceptibility in T2DM patients: A total of 101 patients with both T2DM and malignant tumors (54 males and 47 females) were randomly selected from the Department of Endocrinology and Oncology at the First Affiliated Hospital of Harbin Medical University. Basic information of the patients, such as name, age, gender, and tumor type, was recorded. To evaluate the cancer susceptibility in patients with T2DM, we applied the Significant Bias Evaluation Method using relative risk (RR) and the φ coefficient to assess disease co-occurrence bias. The observed cancer distribution in T2DM patients was compared against 10,000 randomly generated datasets of the same sample size and tumor type distribution. The probability of observing such co-occurrence under random conditions was computed. Bonferroni correction was applied for multiple comparisons, and statistical significance was defined by the adjusted *P*-value [9, 10].

Network distance-based analysis of T2DM and cancer gene set associations: To evaluate the potential associations between T2DM and various cancers, we calculated the network-based distance between the T2DM-related gene sets and cancer-related gene sets with the protein-protein interaction (PPI) network using the PPI-weighted Meet/Min (PPM) distance metric proposed by Sora Yoon [11].

The formula is as follows:

$$PMM(A,B) = 1 - \frac{|A \cap B|}{min\{|A|,|B|\}} - \frac{\alpha}{min\{|A|,|B|\}} \cdot max\begin{cases} \sum_{x \in A-B} \frac{\omega \sum_{y \in A \cap B} p(x,y) + \sum_{y \in B-A} p(x,y)}{max(p) \cdot (\omega |A \cap B| + |B - A|)} \\ \sum_{x \in B-A} \frac{\omega \sum_{y \in A \cap B} p(x,y) + \sum_{y \in A-B} p(x,y)}{max(p) \cdot (\omega |A \cap B| + |A - B|)} \end{cases}$$

$$\omega = \frac{min\{|A|,|B|\}}{|A| + |B|}$$

Where p represents the PPI Scores matrix (the adjacency matrix), and α is a network balance factor ranging from 0 to 1, and ω=min(|A|,|B|)/(|A|+|B|).

The PPI network was derived from the STRING database (version 11.5; https://string-db.org). The T2DM-related genes were obtained from the OMIM database, while cancer-related driver genes were sourced from the COSMIC Cancer Gene Census. For each cancer type, 10,000 random gene set pairs (matching the size of the T2DM and cancer gene sets) were generated, and corresponding PPM values were computed. The significance of the observed PPM value was determined by comparing it to the distribution of the random PPM values. The empirical *P*-value was defined as the proportion of random PPM values less than or equal to the actual observed value. Finally, a false discovery rate (FDR) correction was applied to adjust the *P*-values for multiple testing across the 25 cancer types.

Identification of key factors linking T2DM and cancer using STRING PPI network: To identify key genes mediating the relationship between T2DM and cancer, we utilized the STRING PPI network and betweenness centrality to measure the importance of each node in information transfer between the T2DM- and cancer-related gene sets [12]. The more frequently a node lies on the shortest paths between nodes in the two sets, the more critical it is in

mediating the biological connection. Let gene sets A and B represent the T2DM- and cancer-related genes, respectively. The betweenness centrality of node i is defined as follows:

$$BC(i) = \sum_{k \in A} \sum_{j \in B} \frac{\rho(k,i,j)}{\rho(k,j)}, k \neq i \neq j$$

Where ρ(k,i,j) is the total number of shortest paths between nodes k and j that pass through node i, and ρ(k,j) is the number of shortest paths between nodes k and j. All nodes with non-zero BC values were ranked, and the top 10% were defined as key mediator genes bridging T2DM and cancer [13].

Identification of candidate regulators mediating CRC in T2DM using limma differential expression analysis: Based on transcriptomic data from two sample groups, differential expression analysis was performed using the limma package. Genes were considered differentially expressed if they met the following criteria: Adjusted *P*-value (Benjamini-Hochberg correction) ≤ 0.05, and an absolute log fold change (|logFC|) > 1. Differentially expressed probes were first mapped to RNA IDs using the GEOquery package and then converted to gene symbols using the biomaRt package. If a gene corresponded to multiple probes, the average expression value across samples was used as the gene's final expression level. A heatmap of the differentially expressed genes was generated based on the processed expression matrix, highlighting the expression patterns relevant to CRC pathogenesis in the context of T2DM.

Cell experiments

Cell culture: Human CRC cell line HT29 (iCell Bioscience Inc., Suzhou, China) was cultured in DMEM medium (Gibco, Beijing, China) containing 10% fetal bovine serum (Excell Bio, Suzhou, China) and 1% penicillin-streptomycin solution (Beyotime, Shanghai, China). Cells were maintained at 37°C in a humidified incubator filled with 5% CO_2.

Glucose consumption assay: Cell density was adjusted to 1 × 10^6 cells/mL and then seeded into 96-well plates. Complete culture medium containing insulin (10^{-4}, 10^{-5}, 10^{-6}, 10^{-7}, and 10^{-8} mol/L) was added, with six replicates per group. Cells were incubated at 37°C for 12, 24, 36, and 48 hours. After incubation, the complete culture medium was discarded and replaced with serum-free DMEM. The cells were then incubated for an additional 24 h, after which the glucose content in the supernatant was detected using a glucose assay kit (Nanjing Jiancheng Bioengineering Institute, Nanjing, China). Glucose concentration was calculated as follows:

$$\text{Glucose content } (mmol/L) = \frac{A_{measure} - A_{blank}}{A_{standard} - A_{blank}} \times C_{standard} \times \text{Sample dilution times}$$

Where the standard concentration ($C_{standard}$) is 5.55 mmol/L.

Actual glucose consumption = Glucose content in unseeded cell cultures - Glucose content in the supernatant.

MTT assay: After the glucose consumption assay, cells were cultured with the optimal insulin concentration (Novo Nordisk, Tianjin, China) and seeded in a 96-well plate. After incubation, 10 μL of MTT working solution was added to each well and incubated for 4 hours. Upon the formation of formazan crystals, the supernatant was carefully removed without disturbing the purple crystals. Then, 100 μL of formazan solution was added to each well and incubated at 37°C for 15 minutes to fully dissolve the crystals. Absorbance was measured at 570 nm using a microplate reader. Higher OD value indicate greater cell proliferation, whereas lower OD values suggest reduced proliferation.

CCK-8 assay: Cells were seeded into 96-well plates at 100 μL per well and incubated at 37°C with 5% CO_2 for 24 h. After confirming even cell distribution and good morphology, cells were treated with the selected insulin concentrations and exposure times, as previously described. Subsequently, 10 μL of CCK-8 regent (SevenBio, Beijing, China) was added to each well, followed by incubation in a 5% CO_2 incubator at 37°C for 1 h. Absorbance was measured at 450 nm using a microplate reader. Cell viability was calculated according to the following formula:

$$\text{Cell viability} = (OD_{experimental\ group} - OD_{control\ group}) / (OD_{negative\ control\ group} - OD_{blank\ control\ group}) \times 100\%$$

Cell transfection: GSK3β overexpression (GSK3β-oe), knockdown (GSK3β-si), and corre-

Table 1. GSK3β-si and the corresponding control sequences

GSK3β-si negative control	5'-UUCUCCGAACGUGUCACGU-3'
	5'-ACGUGACACGUUCGGAGAA-3'
GSK3β-si-1	5'-GAGAGAAGAUGAUGUAUAA-3'
	5'-UUAUACAUCAUCUUCUCUC-3'
GSK3β-si-2	5'-GGUGUAAGAGAGCUACUAA-3'
	5'-UUAGUAGCUCUCUUACACC-3'
GSK3β-si-3	5'-AGAAGAUGCUGGUGUUCAA-3'
	5'-UUGAACACCAGCAUCUUCU-3'

sponding negative control plasmids were synthesized by SevenBio (Beijing, China) (**Tables 1** and S1). Transfection was performed using Lipofectamine™ 3000 (Invitrogen, CA, USA) according to manufacturer's instructions. The transfection complexes were incubated at room temperature in the dark for 15 minutes, then added to 6-well plates and incubated at 37°C with 5% CO_2 for 24 h. Transfection efficiency was determined by qRT-PCR.

Immunofluorescence assay: Cells were cultured in 24-well plates, fixed with 4% paraformaldehyde (Solarbio, Beijing, China) for 20 min, followed by permeabilization with 0.5% Triton-X (Beyotime, Shanghai, China) for 20 min. After blocking with 1% BSA solution (Beyotime, Shanghai, China) for 1 h, cells were incubated with the primary antibody (Anti-GSK3β) (PTMab, Beijing, China) at a dilution ratio of 1:50 (150 μL per well) overnight at 4°C. The next day, fluorescent secondary antibody (Proteintech, Wuhan, China) was added at a dilution ratio of 1:200 (150 μL per well) and incubated at room temperature in the dark for 1 h. Then, cells were stained with DAPI (Beyotime, Shanghai, China) at room temperature for 30 minutes. Fluorescent images were captured using a fluorescence microscope.

EdU assay: Cells were seeded in 6-well plates and incubated with 500 μL of EdU working solution (Beyotime, Shanghai, China) mixed with 500 μL of complete culture medium. Cells were incubated in a 5% CO_2 incubator at 37°C for 2 h. Then, the cells were fixed with 4% paraformaldehyde at room temperature for 15 min, permeabilized with 0.3% Triton-X for 15 min. According to the kit instructions, 500 μL of EdU reaction solution was added to each well, gently mixed to ensure complete coverage and incubated at room temperature in the dark for 30 min. Subsequently, 1 mL of diluted Hoechst33342 was added to each well for nuclear staining, and the cells were incubated at room temperature in the dark for 10 min. Fluorescence images were captured using a fluorescence microscope.

Colony formation assay: Cells were seeded into 6-well plates at a density of 700-1000 cells per well. The culture medium was replaced every three days, and colony formation was observed. After 14 days, colonies were fixed with 4% paraformaldehyde for 15 min at room temperature and stained with crystal violet staining solution (Beyotime, China) for 20 min. Plates were then imaged and analyzed. The plating efficiency (PE) was calculated using the following formula: PE = (Clone number/Number of inoculated cells) × 100%. A higher PE value indicates a stronger proliferative capacity.

Flow cytometry: Cells were cultured in 6-well plates and digested using EDTA-free trypsin (SevenBio, Beijing, China). A total of 5×10^5 cells were collected and resuspended in 200 μL of 1 × Binding Buffer from the Annexin-FITC/PI Apoptosis Detection kit (SevenBio, Beijing, China). After centrifugation at 300g for 5 min, the supernatant was discarded. Cells were resuspended in 90 μL of 1 × Binding Buffer, followed by the addition of 5 μL of Annexin V-FITC and 5 μL of PI staining solution. The mixture was gently mixed and incubated at room temperature in the dark for 15 min. Samples were analyzed using FACScan flow cytometry (BD Biosciences, CA, USA), and the results were analyzed with FlowJo_v10.8.1.

RNA extraction and qRT-PCR: Total RNA was extracted from cultured cells and tissues using the TRIzol reagent (Thermo Fisher Scientific, MA, USA). Complementary DNA (cDNA) was synthesized using a reverse transcription kit (SevenBio, Beijing, China). To quantify the target genes, cDNA samples were amplified on an ABI 7500 Fast Real-Time Quantitative PCR instrument (Applied Biosystems, CA, USA) using the SYBR qPCR Mix kit (Toyobo Co., Ltd., Osaka, Japan) and gene-specific primers (**Table 2**). All primers were synthesized by SevenBio (Beijing, China). Relative gene expression levels were calculated using the $2^{-\Delta\Delta Ct}$ method, with β-actin serving as the internal reference. The cycle

Table 2. Primers used for qRT-PCR

GSK3β-F	5'-CCGACTAACACCACTGGAAGCT-3'
GSK3β-R	5'-AGGATGGTAGCCAGAGGTGGAT-3'
β-catenin-F	5'-CACAAGCAGAGTGCTGAAGGTG-3'
β-catenin-R	5'-GATTCCTGAGAGTCCAAAGACAG-3'
CyclinD1-F	5'-TCTACACCGACAACTCCATCCG-3'
CyclinD1-R	5'-TCTGGCATTTTGGAGAGGAAGTG-3'
cMyc-F	5'-CCTGGTGCTCCATGAGGAGAC-3'
cMyc-R	5'-CAGACTCTGACCTTTTGCCAGG-3'
β-actin-F	5'-GGGAAATCGTGCGTGACATT-3'
β-actin-R	5'-GGAACCGCTCATTGCCAAT-3'

threshold (Ct) values were used to compute ΔΔCt as follows: $\Delta\Delta Ct=(Ct_{aim}-Ct_{\beta\text{-actin}})_{experimental\ group}-(Ct_{aim}-Ct_{\beta\text{-actin}})_{control\ group}$.

Western blot: Protein samples were separated on 10% PAGE gel (SevenBio, Beijing, China) and transferred onto PVDF membranes (Millipore, Bedford, MA, USA). Membranes were blocked with 5% skim milk (SevenBio, Beijing, China) and incubated overnight with primary antibodies against human GSK3β (PTMab, Beijing, China), human β-catenin (PTMab, Beijing, China), human CyclinD1 (PTMab, Beijing, China), human cMyc (PTMab, Beijing, China), and human β-actin (Abways, Shanghai, China). Following rinsing with TBS-T (SevenBio, Beijing, China), membranes were incubated with secondary antibodies (Proteintech, Wuhan, China). Protein bands were visualized using enhanced chemiluminescence (ECL) reagents (Beyotime, Shanghai, China).

Statistical analysis

All statistical analyses were conducted using GraphPad Prism 9.0 software. Quantitative data were expressed as mean ± standard deviation (SD). Comparisons between the two groups were performed using unpaired two-tailed Student's *t*-tests. For comparisons among multiple groups, one-way analysis of variance (ANOVA) followed by Tukey's post hoc test was applied. For datasets involving multiple time points or two independent variables (e.g., treatment and time), two-way ANOVA followed by Bonferroni's multiple comparison test was employed. For repeated measurements over time, repeated measures ANOVA was applied. A *p*-value < 0.05 was considered statistically significant.

Results

Clinical co-occurrence analysis revealed increased cancer susceptibility in T2DM patients

To determine whether patients with T2DM exhibit preferential co-occurrence with specific cancer types, we analyzed clinical data from 101 patients diagnosed with both T2DM and malignant tumors. As shown in **Figure 1A**, lung cancer (28.7%), breast cancer (16.8%), colon adenocarcinoma (15.8%), rectal adenocarcinoma (12.9%), and pancreatic cancer (10.9%) were significantly overrepresented compared to randomly expected distributions ($P < 0.001$, Bonferroni-corrected). These findings suggest a non-random pattern of tumor distribution in T2DM patients, implicating potential biological links.

Network-based proximity analysis revealed cancers associated with T2DM-related genes

To explore the molecular associations between T2DM and various cancers, we calculated the PMM distance between T2DM-related genes (from OMIM) and driver gene sets of 25 cancer types (from COSMIC) using the STRING PPI network. For each cancer type, 10,000 random samplings were performed to assess statistical significance. As shown in **Figure 1B**, 15 cancer types, including pancreatic, thyroid, hepatocellular, breast, glioma, and lymphoma, showed significantly lower PMM values ($P < 0.05$), suggesting a closer molecular proximity between these cancers and T2DM-associated genes.

Shared pathogenic mediators identified at the T2DM-cancer interface

To identify key mediators linking T2DM and cancer, we analyzed the network betweenness centrality of all nodes and identified 321 genes with high centrality values at the T2DM-cancer interface. We then examined which of these genes overlapped with known T2DM-related pathogenic genes or cancer driver genes. As summarized in **Table 3**, several overlapping genes were identified in cancers such as acute myeloid leukemia (AML), intestinal cancer, breast cancer, glioma, and lymphoma (e.g., INS, IL6, TBC1D4). Additionally, **Table 4** lists key genes that also serve

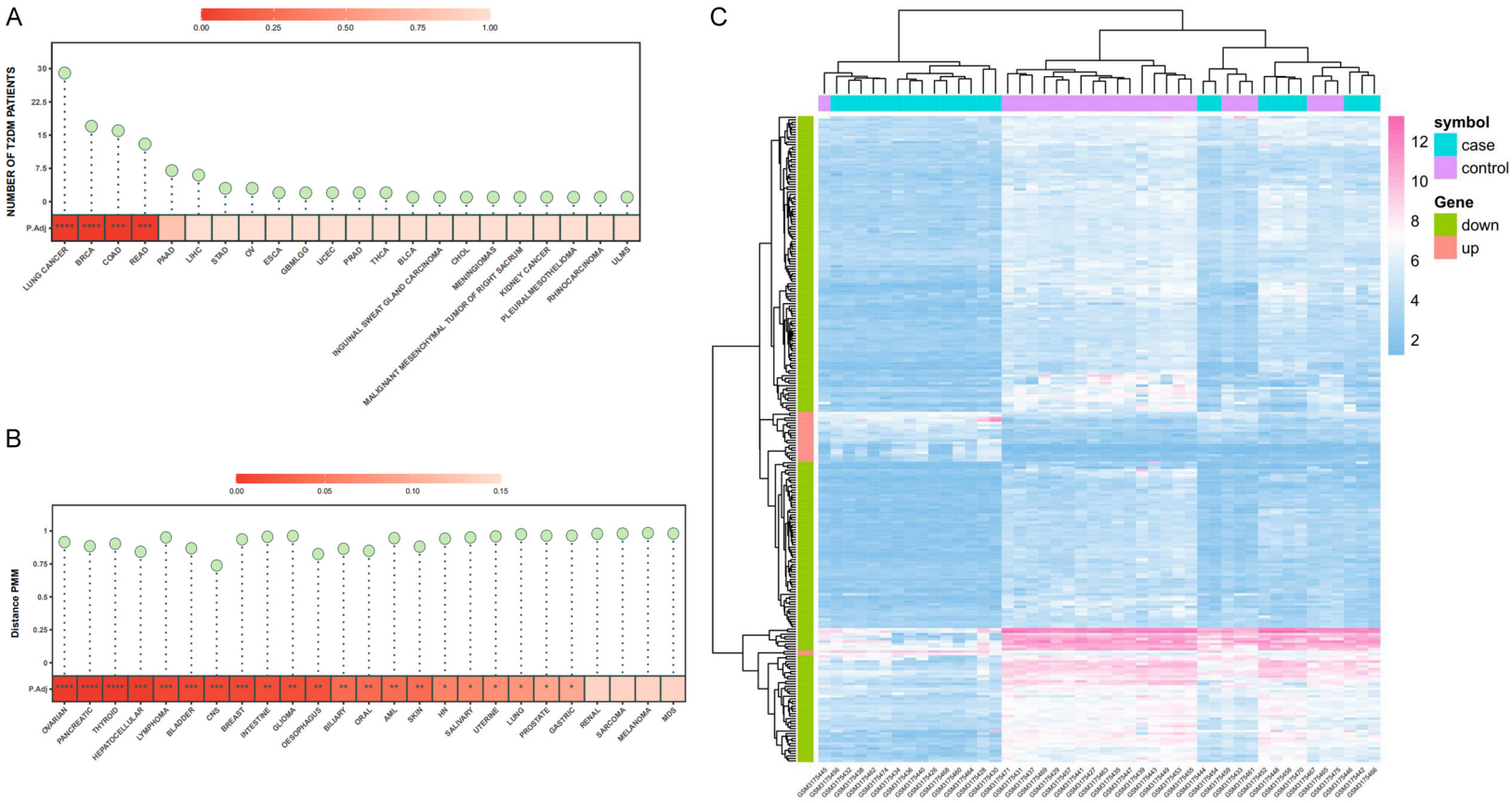

Figure 1. Clinical and molecular associations between T2DM and cancer. A. Clinical co-occurrence analysis shows that lung cancer, breast cancer, colon adenocarcinoma, rectal adenocarcinoma, and pancreatic cancer are significantly overrepresented in T2DM patients compared to random expectations ($P < 0.001$, Bonferroni-corrected). B. Network-based proximity analysis using PMM distance reveals that 15 cancer types, including pancreatic, thyroid, hepatocellular, breast, glioma, and lymphoma, are significantly closer to T2DM-related genes in the STRING PPI network ($P < 0.05$). C. Heatmap showing transcriptomic profiling from GSE115313, where hierarchical clustering of 260 differentially expressed genes distinguishes tumor tissues from adjacent normal tissues in T2DM-associated colorectal cancer patients. GSK3β, a predicted key mediator, is among the significantly dysregulated genes. Data are expressed as mean ± SD. *$P < 0.05$, **$P < 0.01$, ****$P < 0.0001$.

Table 3. Relationship between key genes and disease driver genes

	Both key gene and diabetes pathogenic gene	Both key gene and tumor pathogenic gene
AML	INS, TBC1D4	EP300, RUNX1, JAK2, TCF3, CREBBP, PTPN11, CBL, STAT3, MAPK1, PBX1, BCOR, XPO1, IL7R
INTESTINE	INS, TBC1D4	CTNNB1, EP300, TP53, SRC, ZNRF3, PIK3CA
OVARIAN	INS	CTNNB1
PANCREATIC	INS	EP300
CNS	INS	NF1
SKIN	INS	
LYMPHOMA	INS, TBC1D4	HSP90AA1, IL2, EP300, CLTC, CREBBP, MYH9
GLIOMA	INS	NF1, TP53, EGFR
THYROID	INS	TPR, RET
HEPATOCELLULAR	IL6, INS	
BREAST	INS	EP300, MAP3K1, TP53, RB1, ESR1
BILIARY	INS	
OESOPHAGUS		
BLADDER	INS	
ORAL		

Table 4. Key genes that also serve as pathogenic genes for both T2DM and cancer

Cancer Type	Key Genes Also T2DM Pathogenic Genes	Key Genes Also Cancer Driver Genes
AML	INS, TBC1D4	EP300, RUNX1, JAK2, TCF3, CREBBP, PTPN11, CBL, STAT3, MAPK1, PBX1, BCOR, XPO1, IL7R
Intestine	INS, TBC1D4	CTNNB1, EP300, TP53, SRC, ZNRF3, PIK3CA
Ovarian	INS	CTNNB1
Pancreatic	INS	EP300
CNS	INS	NF1
Skin	INS	-
Lymphoma	INS, TBC1D4	HSP90AA1, IL2, EP300, CLTC, CREBBP, MYH9
Glioma	INS	NF1, TP53, EGFR
Thyroid	INS	TPR, RET
Hepatocellular	IL6, INS	-
Breast	INS	EP300, MAP3K1, TP53, RB1, ESR1
Biliary	INS	-
Esophagus	-	-
Bladder	INS	-
Oral	-	-

as established cancer drivers (e.g., EP300, TP53, CREBBP, EGFR), reinforcing their roles in mediating disease processes. These findings suggest that shared mediators may serve as mechanistic links between T2DM and cancer, potentially explaining the increased cancer susceptibility observed in T2DM patients.

Transcriptomic profiling validated dysregulation of key genes in T2DM-associated colorectal cancer

To confirm whether the predicted key mediators are also dysregulated in clinical samples, we analyzed the GSE115313 dataset, which includes paired tumor and adjacent normal

colorectal tissues from 23 T2DM patients. Differential expression analysis identified 260 significantly dysregulated genes, including 22 upregulated and 238 downregulated ones. As shown in **Figure 1C**, hierarchical clustering of these DEGs revealed distinct separation between tumors and normal tissues. Importantly, GSK3β, one of the predicted key mediators, was significantly upregulated and overlapped with previously identified network hub genes and known T2DM/cancer-related regulators. These results suggest that GSK3β may act as a functional driver of T2DM-associated colorectal tumorigenesis.

Insulin resistance promoted GSK3β expression and enhanced CRC cell proliferation

To investigate whether insulin resistance affects GSK3β expression in CRC, HT29 cells were treated with 10^{-5} mol/L insulin for 24 hours to induce insulin-resistant (IR group), while untreated cells served as controls (NC group). qRT-PCR and Western blot analyses revealed significantly increased GSK3β mRNA and protein expression in IR cells compared to NC cells (**Figure 2A-C**, $P < 0.01$). Immunofluorescence staining further confirmed elevated GSK3β expression in IR cells (**Figure 2D**, $P < 0.01$). Functionally, IR cells exhibited significantly enhanced viability, as shown by CCK-8 assay (**Figure 2E**, $P < 0.0001$), while no significant difference was observed in apoptosis rates between the two groups (**Figure 2F**, $P > 0.05$). To further explore the downstream mechanisms, we assessed the expression of key genes in the proliferation-related pathway. Both mRNA and protein levels of β-catenin, CyclinD1, and cMyc were markedly elevated in IR cells compared to control cells (**Figure 2G**, **2H**, $P < 0.05$ or $P < 0.01$), suggesting that GSK3β may promote CRC proliferation under IR conditions via activation of the β-catenin-CyclinD1/cMyc axis.

GSK3β silencing attenuated, while overexpression enhanced, CRC proliferation via the β-catenin-CyclinD1/cMyc pathway

To validate the functional role of GSK3β in regulating CRC cell proliferation, HT29 IR cells were transfected with wither GSK3β silencing (Si) or overexpression (OE) plasmids. GSK3β-Si-1 exhibited the strongest knockdown efficiency, as confirmed by Western blot and qPCR (**Figure 3A**, **3B**). Compared to negative control (GSK3β-Si-NC), GSK3β knockdown significantly reduced the expression of β-catenin, CyclinD1, and cMyc at both the protein and mRNA levels ($P < 0.01$). Conversely, overexpression of GSK3β (GSK3β-OE group) markedly upregulated these genes compared to the OE control ($P < 0.01$) (**Figure 3C**, **3D**). Immunofluorescence further confirmed the effectiveness of both GSK3β silencing and overexpression at the cellular level (**Figure 3E**, **3F**), supporting its regulatory role in modulating downstream oncogenic targets.

GSK3β regulated CRC cell proliferation under insulin-resistant conditions

To assess the functional role of GSK3β in cell proliferation under IR conditions, we conducted EdU and colony formation assays in HT29 cells. Compared with the NC group, HT29 cells under IR condition exhibited a significantly higher proportion of EdU-positive proliferating cells (**Figure 4A**, $P < 0.0001$), and an increased number of colonies (**Figure 4D**, $P < 0.01$). To further validate the regulatory effect of GSK3β, HT29 cells were transfected with overexpression (GSK3β-OE) or silencing (GSK3β-Si) constructs. GSK3β overexpression significantly promoted proliferation, as indicated by both EdU (**Figure 4B**, $P < 0.001$) and colony assays (**Figure 4E**, $P < 0.01$). Conversely, GSK3β knockdown markedly suppressed proliferation (**Figure 4C-F**, $P < 0.01$). These results suggest that GSK3β is a key promoter of CRC cell proliferation in the context of insulin resistance.

Discussion

In this study, we systematically elucidated the molecular connection between T2DM and cancer, with a particular focus on CRC, by integrating clinical co-occurrence analysis, bioinformatics, and *in vitro* validation. Clinical data from 101 patients with both T2DM and malignancies revealed that lung, breast, colon, rectal, and pancreatic cancers were significantly more prevalent than expected, indicating a non-random distribution of cancer types among T2DM patients. This epidemiological pattern highlights a potential link between metabolic dysregulation and oncogenic processes.

To further explore this association, we conducted a PPI network-based proximity analyses and

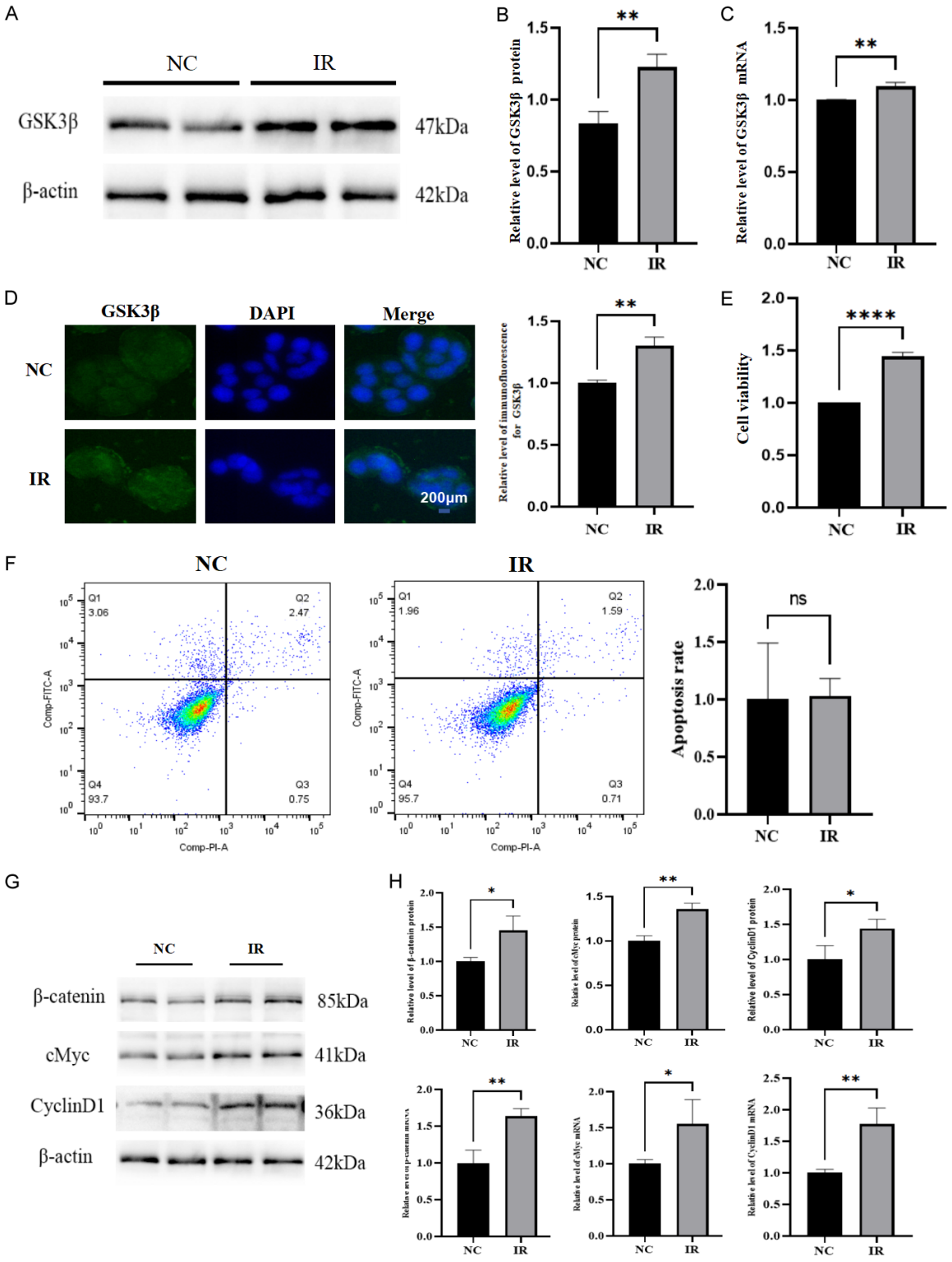

Figure 2. Insulin resistance promoted GSK3β expression and CRC cell proliferation via β-catenin-CyclinD1/cMyc signaling. A-C. qRT-PCR and Western blot showing elevated GSK3β mRNA and protein in IR cells. D. Immunofluorescent intensity of GSK3β was increased in IR cells. E. CCK-8 assay showing increased viability in IR cells compared to NC cells. F. No significant difference in apoptosis rate between IR and NC groups. G, H. β-catenin, CyclinD1, and cMyc mRNA and protein levels are significantly increased in IR vs. NC group. *P < 0.05, **P < 0.01, ****P < 0.0001.

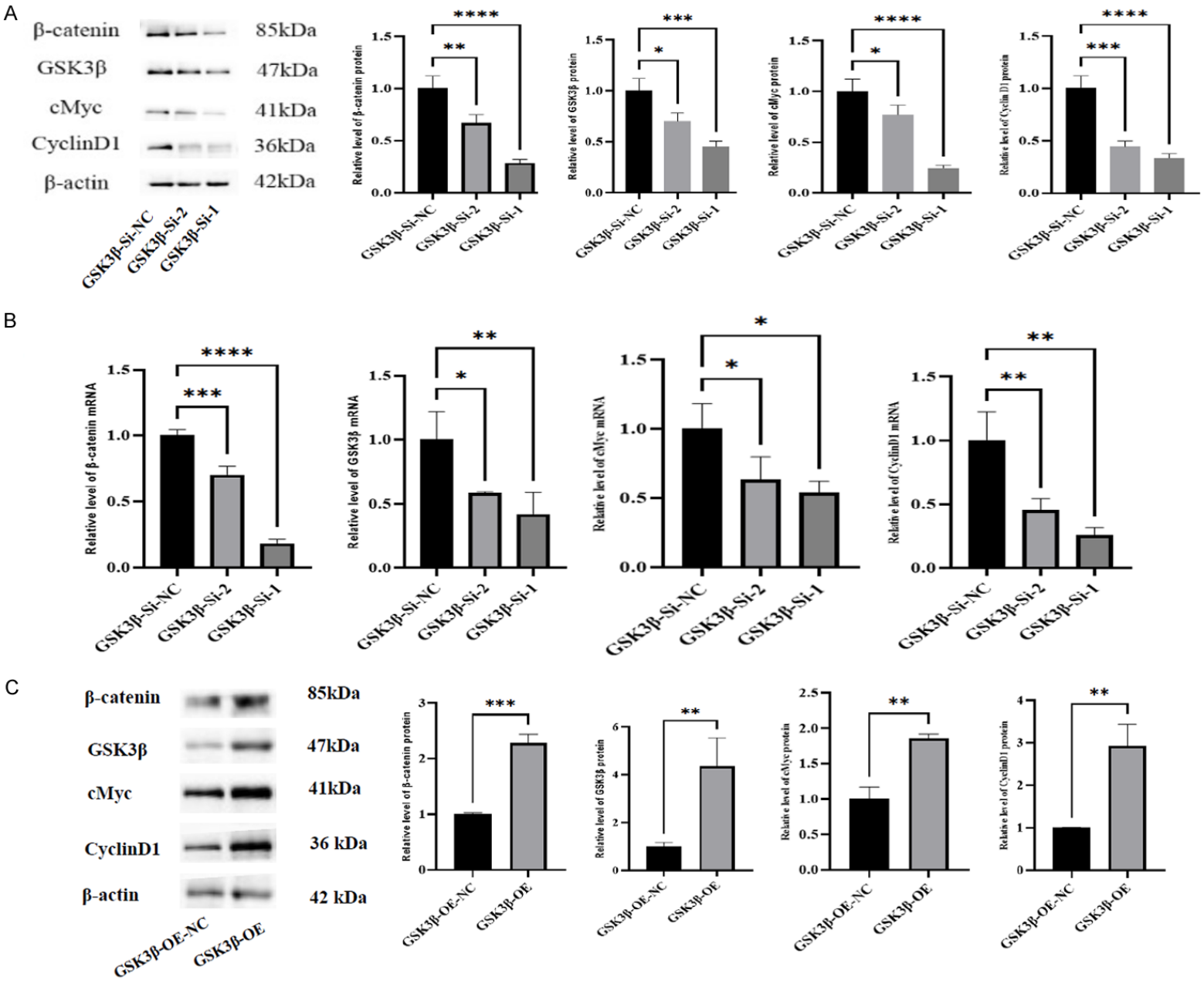
A
β-catenin
GSK3β
cMyc
CyclinD1
β-actin
85kDa
47kDa
41kDa
36kDa
42kDa
GSK3β-Si-NC
GSK3β-Si-2
GSK3β-Si-1
Relative level of β-catenin protein
Relative level of GSK3β protein
Relative level of cMyc protein
Relative level of Cyclin D1 protein
B
Relative level of β-catenin mRNA
Relative level of GSK3β mRNA
Relative level of cMyc mRNA
Relative level of CyclinD1 mRNA
C
β-catenin
GSK3β
cMyc
CyclinD1
β-actin
85kDa
47kDa
41kDa
36 kDa
42 kDa
GSK3β-OE-NC
GSK3β-OE
Relative level of β-catenin protein
Relative level of GSK3β protein
Relative level of cMyc protein
Relative level of CyclinD1 protein

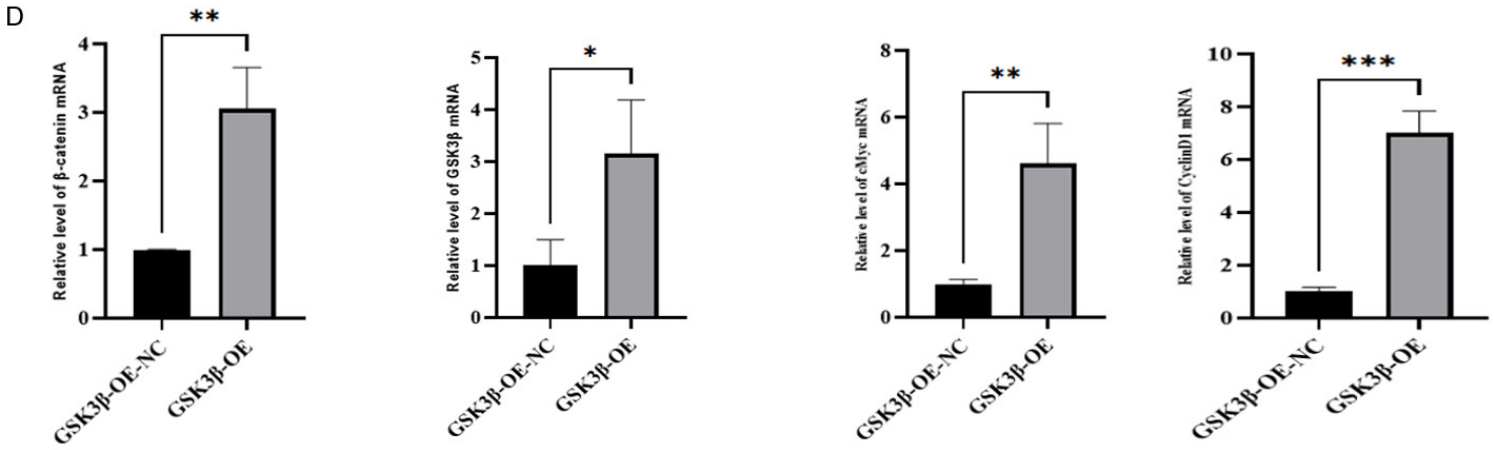
D
Relative level of β-catenin mRNA
Relative level of GSK3β mRNA
Relative level of cMyc mRNA
Relative level of CyclinD1 mRNA
GSK3β-OE-NC
GSK3β-OE

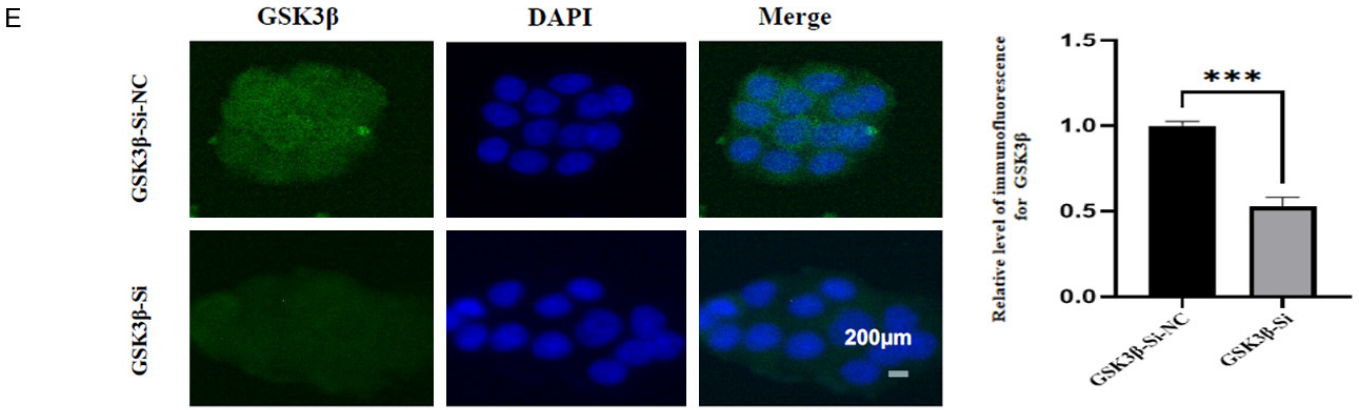
E
GSK3β
DAPI
Merge
GSK3β-Si-NC
GSK3β-Si
200μm
Relative level of immunofluorescence for GSK3β

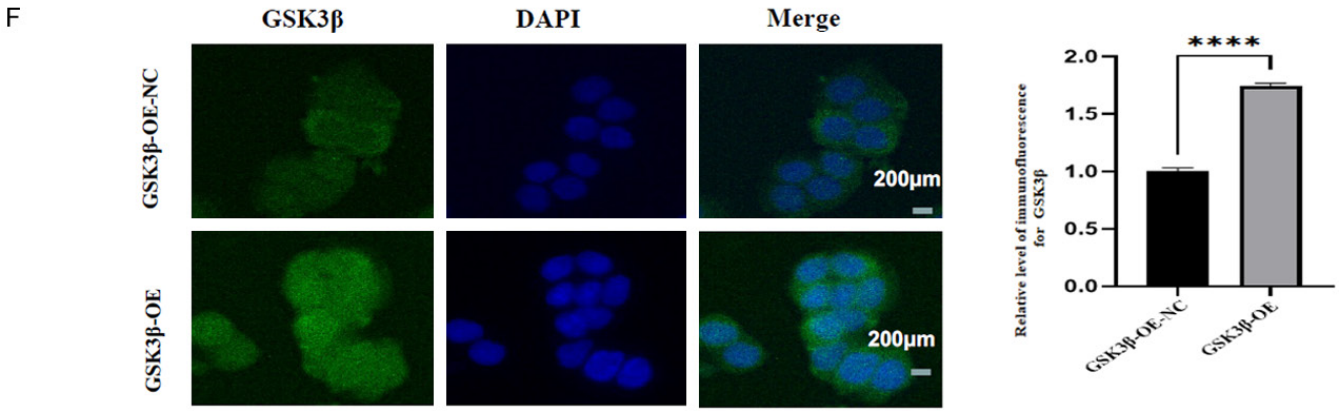
F
GSK3β
DAPI
Merge
GSK3β-OE-NC
GSK3β-OE
200μm
Relative level of immunofluorescence for GSK3β

Figure 3. GSK3β regulated β-catenin-CyclinD1/cMyc expression in insulin-resistant CRC cells. A, B. GSK3β silencing significantly reduced mRNA and protein levels of GSK3β, β-catenin, CyclinD1, and cMyc through western blotting and qRT-PCR. C, D. GSK3β overexpression (OE) significantly upregulated protein and mRNA levels of these targets. E, F. Immunofluorescence shows successful knockdown and overexpression of GSK3β. *P < 0.05, **P < 0.01, ***P < 0.001, ****P < 0.0001.

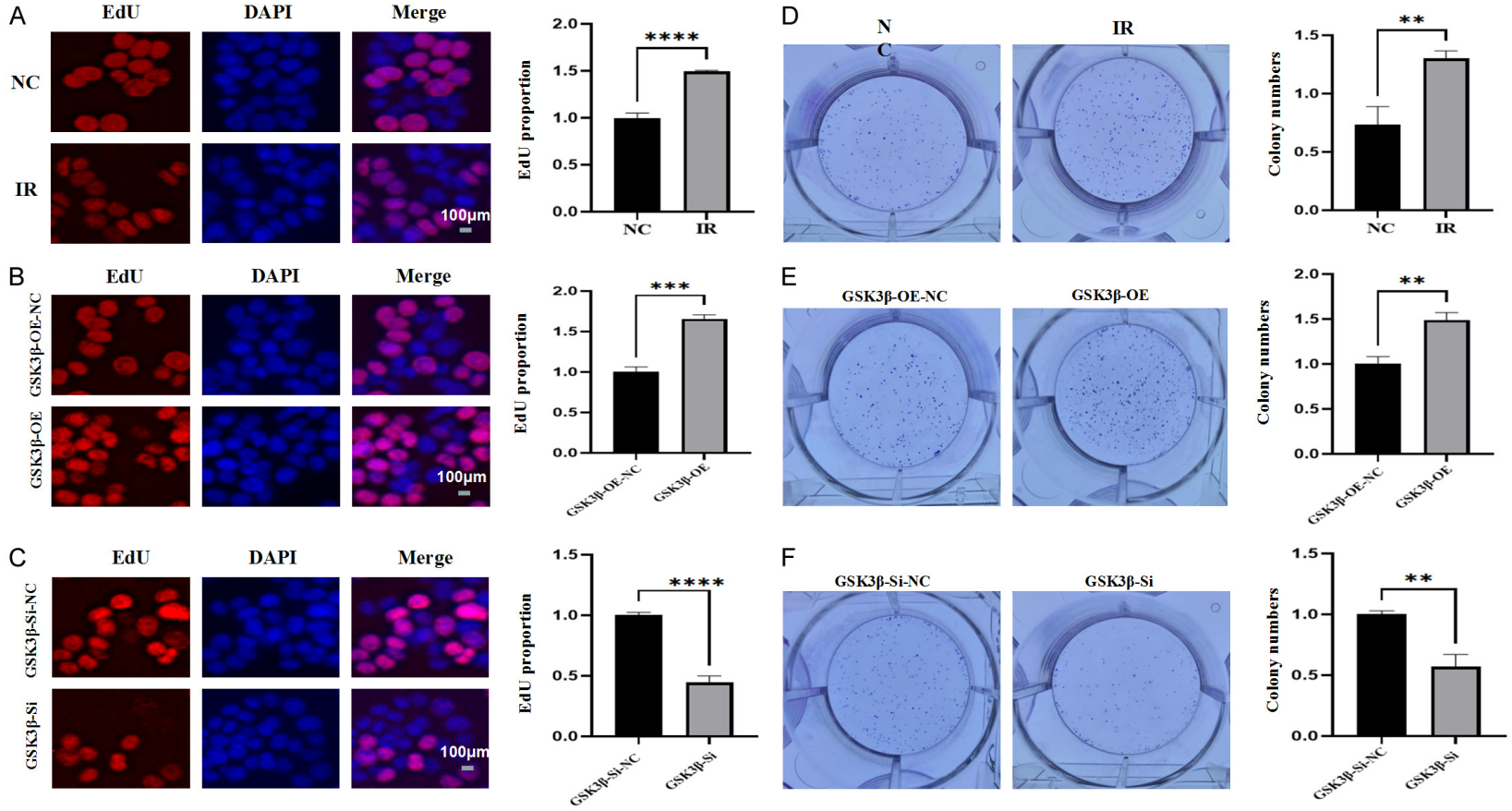

Figure 4. EdU and colony formation assays revealed GSK3β-dependent proliferation in insulin-resistant CRC cells. (A-C) EdU assay shows that proliferation was significantly increased in insulin-resistant CRC cells (A), enhanced in GSK3β overexpression group (B), and decreased in GSK3β-silenced group (C). (D-F) Colony formation assay confirms that cell proliferation was significantly promoted by insulin resistance (D) and GSK3β overexpression (E), while reduced by GSK3β knockdown (F). **P < 0.01, ***P < 0.001, ****P < 0.0001.

identified 15 cancers with significant molecular proximity to T2DM-related genes. This aligns with the perspective of Parvin Mirmiran et al. [14], reinforcing the hypothesis that T2DM and cancer may share common molecular pathways. Using network topology measures, we identified 321 key mediators at the T2DM-cancer interface. Among these, several genes overlapped with known T2DM-related or cancer driver genes, suggesting their potential roles as critical nodes facilitating metabolic-oncogenic crosstalk.

Subsequent transcriptomic validation using the GSE115313 dataset revealed significant differential expression patterns between tumor and adjacent normal tissues in CRC patients T2DM. These molecular alterations are consistent with previous clinical observations. For instance, epidemiological studies have reported that T2DM patients undergoing insulin therapy for at least 3 years had a threefold increased risk of developing CRC compared to non-users, and those treated for ≤ 5 years had a fourfold higher risk [15, 16]. This supports our findings that the development of CRC in T2DM patients is associated with insulin resistance. A meta-analysis of 8 cohort studies from the Knowledge database also revealed a positive correlation between T2DM and the risk of CRC, with a summary relative risk of 1.21-fold [17], further substantiating the association between T2DM and CRC risk.

Notably, GSK3β emerged as a differentially expressed gene, overlapping both with network key mediators and known T2DM- or cancer-related genes. Numerous studies have demonstrated that GSK3β plays complex and context-dependent roles in tumor biology and insulin resistance. For instance, GSK3β has been shown to interfere with insulin signaling by phosphorylating insulin receptor substrate 1 (IRS-1), leading to insulin resistance. Increased GSK3β activity in the skeletal muscle of T2DM patients may also be associated with impaired insulin sensitivity [18-20]. These findings further support our results, suggesting a mechanistic link between GSK3β activity and the pathophysiology of both T2DM and cancer.

Research has also demonstrated that GSK3β inhibitors, when used in combination with other agents, effectively reduce tumor growth and metastasis in pancreatic cancer models [21]. In a 2025 study, Wang et al. reported that adipocyte-specific deletion of GSK3β mice exhibited reduced inflammation, improved insulin sensitivity, and a more favorable microenvironment [22]. In pancreatic cancer, oncogenic KRAS has been shown to drive GSK3β transcription, thereby promoting tumor cell proliferation, survival, and chemotherapy resistance [23]. Moreover, GSK3β inhibition has been shown to selectively suppress tumor growth in FHIT deficient lung cancer [24]. These converging lines of evidence underscore GSK3β as a potential hub gene linking metabolic dysfunction with tumor progression, particularly relevant in CRC development among T2DM patients.

In support of this, our findings suggest that GSK3β may serve as a critical regulator mediating CRC development in T2DM, holding significant biological relevance. Previous studies have established T2DM as a significant risk factor for CRC development, with longer T2DM duration associated with greater CRC risk [25-27]. Additionally, gut microbiota dysbiosis in diabetic patients may exacerbate CRC risk, while shared risk factors such as high-sugar diets and obesity further contribute to CRC susceptibility in this population [28-30].

In 2020, a study published in *Biochimica et Biophysica Acta* (BBA) reported that GSK3β plays complex roles in the proliferation, migration, and apoptosis of tumor cells [31]. In some cancers, GSK3β acts as a tumor suppressor. For example, in mantle cell lymphoma (MCL), GSK3β promotes the degradation of cyclin D1 via phosphorylation, thereby inhibiting tumor cell proliferation [32]. In contrast, in other tumors, GSK3β may promote tumorigenesis through its interaction with oncogenic signaling pathways. For instance, in glioblastoma (GBM), the loss of NDRG1 upregulates GSK3β and enhances cell proliferation [33-35]. Furthermore, Walz et al. proposed that GSK3β functioned as a positive regulator of NF-κB-mediated cancer cell survival. Inhibition of GSK3β reduced the viability of leukemia, pancreatic, and renal cancer cells by downregulating NF-κB target genes such as Bcl-2 and XIAP [36, 37]. These findings align with our experimental data, further supporting the role of GSK3β as critical mediator of tumor cell prolif-

eration, which may underlie the observed interplay between T2DM and CRC.

GSK3β promotes tumor cell proliferation through the GSK3β-β-catenin-CyclinD1/cMyc pathway, thereby promoting tumor initiation and progression [38-40]. Previous studies have indicated that GSK3β can regulate β-catenin activity through multiple mechanisms depending on external stimuli, thereby modulating the expression of downstream genes [23-41]. Therefore, we hypothesized that under insulin-resistant conditions, GSK3β may positively mediate the association between T2DM and CRC through activation of the β-catenin-CyclinD1/cMyc pathway. To test this hypothesis, we established an IR CRC cell model and found that GSK3β expression was significantly upregulated under IR conditions, accompanied by enhanced cell viability and elevated expression of β-catenin, CyclinD1, and cMyc, indicating the activation of a proliferative signaling axis which was consistent with the literature [42-44]. Furthermore, GSK3β knockdown significantly reduced the expression of β-catenin pathway related genes, while overexpression had the opposite effect. Functional assays, including EdU and colony formation, confirmed that GSK3β promotes CRC cell proliferation under IR conditions.

This study has several limitations. First, the sample size for clinical co-occurrence analysis was relatively small, which may limit the generalizability of the findings. Second, *in vitro* validation was conducted in a single colorectal cancer cell line (HT29); additional studies in multiple cell lines and cancer types are needed to verify the broader applicability of the results. Third, no *in vivo* experiments were conducted, leading the systemic effects of IR on tumor progression unaddressed. Future studies should incorporate larger clinical datasets and animal models to validate the role of GSK3β in T2DM-related cancers. Moreover, the therapeutic potential of targeting GSK3β in diabetic patients at elevated cancer risk warrants further investigation.

Together, our results provide mechanistic insights into how insulin resistance - a hallmark feature of T2DM - may contribute to CRC progression via GSK3β-mediated signaling. Unlike prior studies that have focused primarily on epidemiological associations, this work integrates computational predictions with experimental validation, establishing GSK3β as a key molecular bridge between metabolic dysfunction and oncogenic progression. These findings pave the way for future therapeutic strategies targeting GSK3β in managing T2DM-associated cancers.

Conclusion

GSK3β expression is increased in CRC with T2DM, promoting proliferation and aggravates tumor development and progression. GSK3β is expected to be a new biological target for the treatment of T2DM patients with CRC and provide help to solve practical problems clinically.

Acknowledgements

This research was supported by the National Natural Science Foundation of China (Grant No. 62172128), Shenzhen Science and Technology Plan Basic Research (General Project) project-JCYJ20210324103610029 and Joint project of Institute of Biophysics, Chinese Academy of Sciences: establishment of prospective biobank of Chinese population 1 million KJDZ-EW-TZ-L05 2016.01-2020.12. We are grateful for their support.

Disclosure of conflict of interest

None.

Address correspondence to: Xiaorong Zhan, Department of Endocrinology, The First Affiliated Hospital of Harbin Medical University, Harbin 150001, Heilongjiang, China. E-mail: xiaorongzhan1114@126.com

References

[1] Vulichi SR, Runthala A, Begari N, Rupak K, Chunduri VR, Kapur S, Chippada AR and Sistla DSM. Type-2 diabetes mellitus-associated cancer risk: in pursuit of understanding the possible link. Diabetes Metab Syndr 2022; 16: 102591.

[2] Chen L, Zhou Y, Yan G, Shen Y, Sun C, Cai W, Chu M and Xiao J. Risk of malignant tumor in patients with type 2 diabetes: a prospective population-based study. Chinese General Practice 2023; 26: 3238-3245.

[3] Pearson-Stuttard J, Bennett J, Cheng YJ, Vamos EP, Cross AJ, Ezzati M and Gregg EW. Trends in predominant causes of death in indi-

viduals with and without diabetes in England from 2001 to 2018: an epidemiological analysis of linked primary care records. Lancet Diabetes Endocrinol 2021; 9: 165-173.
[4] Huan W. Analysis and mechanism of patients with type 2 diabetes in Changchun. The First Bethune Hospital Jilin University; 2023. [Thesis].
[5] Pan XF, He M, Yu C, Lv J, Guo Y, Bian Z, Yang L, Chen Y, Wu T, Chen Z, Pan A and Li L; China Kadoorie Biobank Collaborative Group. Type 2 diabetes and risk of incident cancer in China: a prospective study among 0.5 million Chinese adults. Am J Epidemiol 2018; 187: 1380-1391.
[6] Wei W, Zeng H, Zheng R, Zhang S, An L, Chen R, Wang S, Sun K, Matsuda T, Bray F and He J. Cancer registration in China and its role in cancer prevention and control. Lancet Oncol 2020; 21: e342-e349.
[7] Nunes L, Li F, Wu M, Luo T, Hammarström K, Torell E, Ljuslinder I, Mezheyeuski A, Edqvist PH, Löfgren-Burström A, Zingmark C, Edin S, Larsson C, Mathot L, Osterman E, Osterlund E, Ljungström V, Neves I, Yacoub N, Guðnadóttir U, Birgisson H, Enblad M, Ponten F, Palmqvist R, Xu X, Uhlén M, Wu K, Glimelius B, Lin C and Sjöblom T. Prognostic genome and transcriptome signatures in colorectal cancers. Nature 2024; 633: 137-146.
[8] Wolf AMD, Fontham ETH, Church TR, Flowers CR, Guerra CE, LaMonte SJ, Etzioni R, McKenna MT, Oeffinger KC, Shih YT, Walter LC, Andrews KS, Brawley OW, Brooks D, Fedewa SA, Manassaram-Baptiste D, Siegel RL, Wender RC and Smith RA. Colorectal cancer screening for average-risk adults: 2018 guideline update from the American cancer society. CA Cancer J Clin 2018; 68: 250-281.
[9] Sioutos N, de Coronado S, Haber MW, Hartel FW, Shaiu WL and Wright LW. NCI thesaurus: a semantic model integrating cancer-related clinical and molecular information. J Biomed Inform 2007; 40: 30-43.
[10] Žitnik M, Janjić V, Larminie C, Zupan B and Leskovec J. Discovering disease-disease associations by fusing systems-level molecular data. Sci Rep 2013; 3: 3202.
[11] Yoon S, Kim J, Kim SK, Baik B, Chi SM, Kim SY and Nam D. GScluster: network-weighted gene-set clustering analysis. BMC Genomics 2019; 20: 352.
[12] Kivimäki I, Lebichot B, Saramäki J and Saerens M. Two betweenness centrality measures based on randomized shortest paths. Sci Rep 2016; 6: 19668.
[13] Li X, Li W, Zeng M, Zheng R and Li M. Network-based methods for predicting essential genes or proteins: a survey. Brief Bioinform 2020; 21: 566-583.
[14] Camps-Fajol C, Cavero D, Minguillón J and Rabal O. Targeting protein-protein interactions in drug discovery: modulators approved or in clinical trials for cancer treatment. Pharmacol Res 2025; 211: 107544.
[15] Carr PR, Weigl K, Edelmann D, Jansen L and Hoffmeister M. Estimation of absolute risk of colorectal cancer based on healthy lifestyle, genetic risk, and colonoscopy status in a population-based study. Gastroenterology 2020; 159: 129-138, e9.
[16] Guraya SY. Association of type 2 diabetes mellitus and the risk of colorectal cancer: a meta-analysis and systematic review. World J Gastroenterol 2015; 21: 6026-6031.
[17] Miao S, Song J, Liu Q, Sun Y and Zhang H. Integrated bioinformatics analysis to identify the key gene associated with metastatic clear cell renal cell carcinoma. Med Oncol 2022; 39: 128.
[18] Ciaraldi TP, Nikoulina SE, Bandukwala RA, Carter L and Henry RR. Role of glycogen synthase kinase-3 alpha in insulin action in cultured human skeletal muscle cells. Endocrinology 2007; 148: 4393-4399.
[19] Lappas M. GSK3β is increased in adipose tissue and skeletal muscle from women with gestational diabetes where it regulates the inflammatory response. PLoS One 2014; 9: e115854.
[20] Zhu B, Wu X, Wu B, Pei D and Zhang L. The relationship between diabetes and colorectal cancer prognosis: a meta-analysis based on the cohort studies. PLoS One 2017; 12: e0176068.
[21] Henriksen EJ and Dokken BB. Role of glycogen synthase kinase-3 in insulin resistance and type 2 diabetes. Curr Drug Targets 2006; 7: 1435-1441.
[22] Ding L and Billadeau DD. Glycogen synthase kinase-3β: a novel therapeutic target for pancreatic cancer. Expert Opin Ther Targets 2020; 24: 417-426.
[23] Tao S, Pu Y, Yang EJ, Ren G, Shi C, Chen LJ, Chen L and Shim JS. Inhibition of GSK3β is synthetic lethal with FHIT loss in lung cancer by blocking homologous recombination repair. Exp Mol Med 2025; 57: 167-183.
[24] Li J, Tao S, Cong L, Chen J and Zhao H. GSK-3β in DNA repair, apoptosis, and resistance of chemotherapy, radiotherapy of cancer. Biochim Biophys Acta Mol Cell Res 2020; 1867: 118659.
[25] Herold M, Szasz AM, Szentmartoni G, Dank M and Hegedus B. Influence of the duration of type 2 diabetes mellitus on colorectal cancer outcomes. Sci Rep 2023; 13: 12985.
[26] Farahani H, Mahmoudi T, Asadi A, Nobakht H, Dabiri R and Hamta A. Insulin resistance and colorectal cancer risk: the role of elevated

plasma resistin levels. J Gastrointest Cancer 2020; 51: 478-483.
[27] Baban B, Eklund D, Tuerxun K, Abdugheni R and Khamjan M. Altered insulin sensitivity and immune function in patients with colorectal cancer. Clin Nutr ESPEN 2023; 58: 193-200.
[28] Li W, Liu T, Qian L, Zhang X and Huang G. Insulin resistance and inflammation mediate the association of abdominal obesity with colorectal cancer risk. Front Endocrinol (Lausanne) 2022; 13: 983160.
[29] Domoto T, Pyko IV, Furuta T, Miyashita K, Uehara M, Shimasaki T, Nakada M and Minamoto T. Glycogen synthase kinase-3β is a pivotal mediator of cancer invasion and resistance to therapy. Cancer Sci 2016; 107: 1363-1372.
[30] Wang L, Li J, Tang P, Liu F and Song X. GSK3β deficiency expands obese adipose vasculature to mitigate metabolic disorders. Circ Res 2025; 136: 91-111.
[31] Samara A, Shapira S, Lubin I, Ben-Ami O and Nassar T. Deferasirox induces cyclin D1 degradation and apoptosis in mantle cell lymphoma in a reactive oxygen species- and GSK3β-dependent mechanism. Br J Haematol 2021; 192: 747-760.
[32] He R, Du S, Lei T, Zhang A and Wang Y. Glycogen synthase kinase 3β in tumorigenesis and oncotherapy (Review). Oncol Rep 2020; 44: 2373-2385.
[33] Duda P, Akula SM, Abrams SL, Steelman LS and Martelli AM. Targeting GSK3 and associated signaling pathways involved in cancer. Cells 2020; 9: 1110.
[34] Ito H, Watari K, Shibata T, Murakami Y and Yamasaki T. Bidirectional regulation between NDRG1 and GSK3β controls tumor growth and is targeted by differentiation inducing factor-1 in glioblastoma. Cancer Res 2020; 80: 234-248.
[35] Shu Q, Liu J, Liu X, Zhang Q and Chen H. GABAB R/GSK-3β/NF-κB signaling pathway regulates the proliferation of colorectal cancer cells. Cancer Med 2016; 5: 1259-1267.
[36] Walz A, Ugolkov A, Chandra S, Abdulkadir SA and Giles FJ. Molecular pathways: revisiting glycogen synthase kinase-3β as a target for the treatment of cancer. Clin Cancer Res 2017; 23: 1891-1897.
[37] Zhou J, Wang X, Li Z, Chen Y and Zhang W. PIM1 kinase promotes EMT-associated osimertinib resistance via regulating GSK3β signaling pathway in EGFR-mutant non-small cell lung cancer. Cell Death Dis 2024; 15: 644.
[38] Wang J, Su W, Zhang T, Liu J and Chen Q. Aberrant cyclin D1 splicing in cancer: from molecular mechanism to therapeutic modulation. Cell Death Dis 2023; 14: 244.
[39] Fatma H, Maurya SK and Siddique HR. Epigenetic modifications of c-MYC: role in cancer cell reprogramming, progression and chemoresistance. Semin Cancer Biol 2022; 83: 166-176.
[40] Teli DM and Gajjar AK. Glycogen synthase kinase-3: a potential target for diabetes. Bioorg Med Chem 2023; 92: 117406.
[41] Liu J, Xiao Q, Xiao J, Zhang L and Wang Y. Wnt/β-catenin signalling: function, biological mechanisms, and therapeutic opportunities. Signal Transduct Target Ther 2022; 7: 3.
[42] Zhou Z, Li Y, Chai Y, Liu Y and Huang J. Analysis of mRNA pentatricopeptide repeat domain 1 as a prospective oncogene in clear cell renal cell carcinoma that accelerates tumor cells proliferation and invasion via the Akt/GSK3β/β-catenin pathway. Discov Oncol 2025; 16: 22.
[43] Shakoori A, Mai W, Miyashita K, Yasumoto K and Takebayashi S. Inhibition of GSK-3β activity attenuates proliferation of human colon cancer cells in rodents. Cancer Sci 2007; 98: 1388-1393.
[44] O'Connor MJ, Thakar T, Nicolae CM, Lin YL and Moldovan GL. PARP14 regulates cyclin D1 expression to promote cell-cycle progression. Oncogene 2021; 40: 4872-4883.

Table S1. GSK3β-oe sequence

GCTAGCATGTCAGGGCGGCCCAGAACCACCTCCTTTGCGGAGAGCTGCAAGCCGGTGCAGCAGCCTTCAGCTTTTGGCAG- CATGAAAGTTAGCAGAGACAAGGACGGCAGCAAGGTGACAACAGTGGTGGCAACTCCTGGGCAGGGTCCAGACAGGCCA- CAAGAAGTCAGCTATACAGACACTAAAGTGATTGGAAATGGATCATTTGGTGTGGTATATCAAGCCAAACTTTGTGATTCAGGAGA- ACTGGTCGCCATCAAGAAAGTATTGCAGGACAAGAGATTTAAGAATCGAGAGCTCCAGATCATGAGAAAGCTAGATCACTGTAA- CATAGTCCGATTGCGTTATTTCTTCTACTCCAGTGGTGAGAAGAAAGATGAGGTCTATCTTAATCTGGTGCTGGACTATGTTCCG- GAAACAGTATACAGAGTTGCCAGACACTATAGTCGAGCCAAACAGACGCTCCCTGTGATTTATGTCAAGTTGTATATGTATCAGCT- GTTCCGAAGTTTAGCCTATATCCATTCCTTTGGAATCTGCCATCGGGATATTAAACCGCAGAACCTCTTGTTGGATCCTGATACT- GCTGTATTAAAACTCTGTGACTTTGGAAGTGCAAAGCAGCTGGTCCGAGGAGAACCCAATGTTTCGTATATCTGTTCTCGGTAC- TATAGGGCACCAGAGTTGATCTTTGGAGCCACTGATTATACCTCTAGTATAGATGTATGGTCTGCTGGCTGTGTGTTGGCTGAGCT- GTTACTAGGACAACCAATATTTCCAGGGGATAGTGGTGTGGATCAGTTGGTAGAAATAATCAAGGTCCTGGGAACTCCAA- CAAGGGAGCAAATCAGAGAAATGAACCCAAACTACACAGAATTTAAATTCCCTCAAATTAAGGCACATCCTTGGACTAAGGATTC- GTCAGGAACAGGACATTTCACCTCAGGAGTGCGGGTCTTCCGACCCCGAACTCCACCGGAGGCAATTGCACTGTGTAGCCGTCT- GCTGGAGTATACACCAACTGCCCGACTAACACCACTGGAAGCTTGTGCACATTCATTTTTTGATGAATTACGGGACCCAAATGT- CAAACTACCAAATGGGCGAGACACACCTGCACTCTTCAACTTCACCACTCAAGAACTGTCAAGTAATCCACCTCTGGCTACCATCCT- TATTCCTCCTCATGCTCGGATTCAAGCAGCTGCTTCAACCCCCACAAATGCCACAGCAGCGTCAGATGCTAATACTGGAGACCGTG- GACAGACCAATAATGCTGCTTCTGCATCAGCTTCCAACTCCACCTGACTCGAG